

Local nematic susceptibility in stressed BaFe₂As₂ from NMR electric field gradient measurements

T. Kissikov,¹ R. Sarkar,² M. Lawson,¹ B. T. Bush,¹ E. I. Timmons,³ M. A. Tanatar,³ R. Prozorov,³ S. L. Bud'ko,³ P. C. Canfield,³ R. M. Fernandes,⁴ W. F. Goh,¹ W. E. Pickett,¹ and N. J. Curro¹

¹*Department of Physics, University of California, Davis, California 95616, USA*

²*Institute for Solid State Physics, TU Dresden, D-01069 Dresden, Germany*

³*Ames Laboratory U.S. DOE and Department of Physics and Astronomy, Iowa State University, Ames, Iowa 50011, USA*

⁴*School of Physics and Astronomy, University of Minnesota, Minneapolis, Minnesota 55455, USA*

(Dated: October 20, 2017)

The electric field gradient (EFG) tensor at the ⁷⁵As site couples to the orbital occupations of the As p-orbitals and is a sensitive probe of local nematicity in BaFe₂As₂. We use nuclear magnetic resonance to measure the nuclear quadrupolar splittings and find that the EFG asymmetry responds linearly to the presence of a strain field in the paramagnetic phase. We extract the nematic susceptibility as a function of temperature and find that it diverges near the structural transition in agreement with other measures of the global susceptibility.

PACS numbers: 76.60.-k, 75.30.Mb, 75.25.Dk, 76.60.Es

The iron-based superconductors exhibit a complex interplay between orbital, electronic and lattice degrees of freedom. In BaFe₂As₂ a ferro-orbital instability is accompanied by an orthorhombic distortion and long-range antiferromagnetic order [1, 2]. This nematic phase breaks the C₄ tetragonal symmetry of the lattice, and is preceded by critical nematic fluctuations and divergent nematic susceptibility in the disordered phase [3, 4]. In the nematic phase, the Fe *d_{xz}* and *d_{yz}* orbitals become non-degenerate, with an energy splitting on the order of 40 meV, and different occupation levels [5]. This phase also stabilizes antiferromagnetic ordering of the Fe spins, which order either concomitantly with the nematic phase transition, or at a temperature *T_N* only a few Kelvins below. As a result, many low energy experimental probes actually sense a complex interplay of the orbital, lattice, and magnetic degrees of freedom simultaneously, precluding quantitative analyses.

Several techniques have been developed to probe the nematic degrees of freedom. Anisotropic resistivity [6, 7], elastoresistance [3], electronic Raman scattering [8], elastic constants [9–11], thermopower, polarized light image color analysis [12, 13] and optical conductivity [14] probe global, macroscopic anisotropies. NMR and neutron scattering, on the other hand, are microscopic probes, and have been used to investigate the effect of nematicity on the spin fluctuations [15–19]. The nuclear quadrupolar interaction, however, can probe the microscopic orbital occupations directly [20]. The ⁷⁵As (*I* = 3/2) quadrupolar moment couples to the local electric field gradient (EFG), which is dominated by the on-site occupations of the As 4p electrons. These orbitals are hybridized with the Fe 3d orbitals, and thus the EFG is a sensitive probe of the d-orbital occupations. Indeed, the EFG tensor exhibits a dramatic lowering from axial symmetry at the nematic phase transition in the absence of applied strain [21]. In this Rapid Communication we

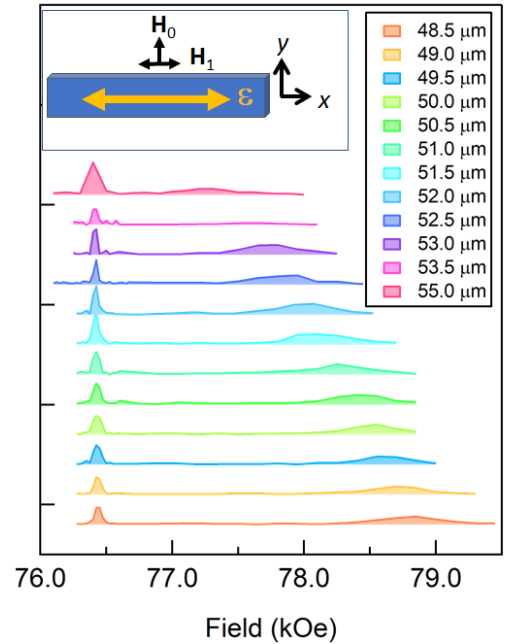


FIG. 1. (color online) Field-swept spectra of BaFe₂As₂ at constant frequency *f* = 55.924 MHz at 138 K for several different displacements of the piezoelectric device, showing the central and upper satellite transitions. INSET: Orientation of the crystal with respect to the external field, **H**₀, the strain axis, and the rf field **H**₁.

present new data on the EFG under uniaxial strain. We find that the EFG asymmetry parameter is linearly proportional to the in-plane strain applied to the crystal, and is a direct measure of the nematic susceptibility. This approach enables one to probe the *local*, rather than global, nematic susceptibility.

A single crystal of BaFe₂As₂ was synthesized via a self-flux method and cut to dimensions of approximately 1.5

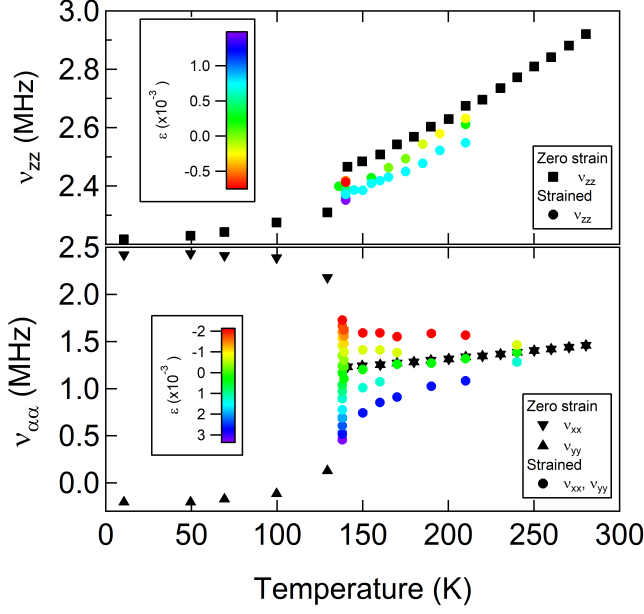


FIG. 2. (color online) The electric field gradient components (ν_{xx} , ν_{yy} , ν_{zz}) for the As versus temperature for BaFe₂As₂ both in zero strain (reproduced from [21]) and under uniaxial strain.

mm \times 0.5 mm with the long axis parallel to the (110)_T direction in the tetragonal basis along the Fe-Fe bond direction. The sample was mounted in a custom-built NMR probe incorporating a Razorbill cryogenic strain apparatus [22]. Uniaxial stress was applied to the crystal as described in [16] by piezoelectric stacks as illustrated in the inset of Fig. 1, and strain was measured by a capacitive dilatometer. A free-standing NMR coil was placed around the crystal, and spectra were measured by acquiring echoes while sweeping the magnetic field H_0 at fixed frequency, as shown in Fig. 1. ⁷⁵As has spin $I = 3/2$, with three separate resonances separated by the quadrupolar interaction. The higher quadrupolar satellite resonance occurs at field $H_{sat} = (f_0 + \nu_{\alpha\alpha})/\gamma(1 + K_{\alpha\alpha})$, where $f_0 = 55.924$ MHz is the rf frequency, $\gamma = 7.29019$ MHz/T is the gyromagnetic ratio, and $K_{\alpha\alpha}$ and $\nu_{\alpha\alpha}$ are the Knight shift and EFG tensor components in the $\alpha = (x, y, z)$ direction. The central transition field is given by: $H_{cen} = \frac{f_0}{\gamma(1+K_{\alpha\alpha})} \left(\frac{1}{2} + \sqrt{\frac{3f_0^2 - 2(\nu_{\beta\beta} + \nu_{\alpha\alpha})^2}{12}} \right)$, where $\beta = (y, x, z)$ for $\alpha = x, y, z$. The center of gravity of each peak was used to determine the resonance field, and hence $K_{\alpha\alpha}$ and $\nu_{\alpha\alpha}$ as a function of strain. The Knight shift shows essentially no change with strain [16], however, all components of the EFG tensor show strong variations, as shown in Fig. 2 and Fig. 3.

The EFG tensor is given by $\nu_{\alpha\beta} = (eQ/12h)\partial^2V/\partial x_\alpha\partial x_\beta$, where $Q = 3.14 \times 10^{-29}$ m² is the quadrupolar moment of the ⁷⁵As and V is the electrostatic potential at the As site. This quantity is

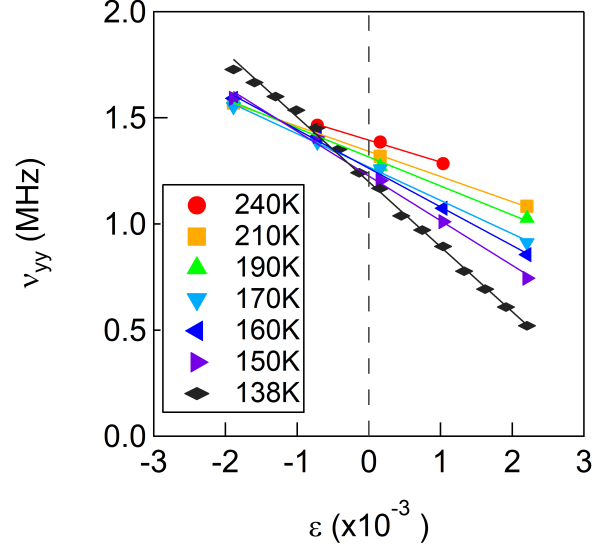


FIG. 3. (color online) The quadrupolar splitting ν_{yy} as a function of strain at several fixed temperatures. The solid lines are linear fits to the data.

dominated by the occupation of the As 4p orbitals, which in turn are hybridized with the $d_{xz,yz}$ -orbitals of the neighboring Fe atoms [20]. In the tetragonal phase the EFG asymmetry parameter $\eta = (\nu_{yy} - \nu_{xx})/(\nu_{xx} + \nu_{yy})$ vanishes, as seen in Fig. 2. In the presence of finite nematicity, the C_4 symmetry of the EFG tensor is broken and $\nu_{xx} \neq \nu_{yy}$ [23]. In-plane anisotropic strain fields, $\varepsilon_{ani} = \frac{1}{2}(\varepsilon_{xx} - \varepsilon_{yy})$, with B_{2g} symmetry (in the coordinate system of the tetragonal unit cell) couple bilinearly to nematicity, therefore η responds to strain in the same manner that the magnetization of a ferromagnet responds to a uniform magnetic field [3, 12, 24]. Due to a finite Poisson ratio, uniaxial stress induces strains $\varepsilon_{\alpha\alpha}$ ($\alpha = x, y, z$) along three different directions, but the dominant contribution is ε_{ani} that couples to η . In our configuration we can only apply \mathbf{H}_0 perpendicular to the stress axis. We measure both $\nu_{zz} = \nu_{cc}$ along the \hat{c} axis of the crystal, and ν_{yy} for \mathbf{H}_0 in the basal plane. For the latter case, $\nu_{yy} = \nu_{aa}$ for compressive strain ($\varepsilon_{ani} < 0$) and $\nu_{yy} = \nu_{bb}$ for tensile strain ($\varepsilon_{ani} > 0$), and $\nu_{xx}(\varepsilon_{ani}) = \nu_{yy}(-\varepsilon_{ani})$. The EFG thus enables us to identify the zero-strain displacement, x_0 , by the condition $|\nu_{xx}| = |\nu_{yy}| = |\nu_{zz}|/2$. Note that η can exceed unity, since $\nu_{xx} + \nu_{yy} + \nu_{zz} = 0$. Furthermore, in the absence of strain a global order parameter in a twinned sample would average to zero, whereas the local order measured by NMR reveals all domains simultaneously [21].

As seen in Fig. 2, the applied strain significantly alters the local EFG. Just above the structural transition $T_s = 135$ K, the strained EFG values approach those in the spontaneously ordered phase in the absence of strain. Furthermore, the maximum strain levels as measured by

the dilatometer reach approximately 60% of the spontaneous values of the orthorhombicity in the ordered phase [25]. Nevertheless, ν_{yy} remains linear over this range as shown in Fig. 3. The slope of this response is therefore a measure of the static nematic susceptibility, χ_{nem} . Similar behavior was observed in elastoresistance [3], shear modulus [11], and electronic Raman scattering [26]. However, the NMR probes the local nematicity in terms of the different orbital occupations obtained from calculated EFGs, rather than the global response due to different nematic domains.

Figure 4 shows the temperature dependence of $d\eta/d\varepsilon_{ani}$ and compares the response to elastoresistance measurements [3]. The NMR data exhibit a similar behavior with a divergence at T_s . We fit the EFG data to the sum of a Curie-Weiss term plus a background susceptibility: $\chi_{\text{nem}} = C/(T-T_0) + \chi_0$, and find $C_0 = 4700 \pm 700$ K, $T_0 = 116 \pm 3$ K, and $\chi_0 = 54 \pm 8$. The background term reflects the intrinsic response of the lattice, whereas the Curie-Weiss term represents the nematic instability. Our observed value of T_0 is consistent with elastoresistance and shear modulus measurements, but differs from that observed by Raman scattering [11, 26, 27]. The difference between T_0 and T_s arises due to the coupling between the electronic nematic and the lattice, so that the free energy instability occurs before the divergence [28].

In order to understand the relationship between the EFG asymmetry and the splitting between the Fe d_{xz} and d_{yz} orbitals, we have performed GGA-based DFT calculations [?] for the tetragonal structure at 300 K and 0.2 GPa [?] under anisotropic in-plane strain ε_{ani} . Our values of the EFG are consistent with previous calculations in the absence of strain, but underestimate the experimental values by approximately a factor of three [29, 30]. We confirm that the EFG is dominated by the occupation of the As p orbitals [20], which are hybridized with the neighboring d_{xz} and d_{yz} orbitals. We calculate that $d\eta/d\varepsilon_{ani} = 33$, which is close to the experimental value of the background susceptibility, χ_0 . The strong temperature-dependent divergence at T_s is a collective phenomenon driven by the electronic system and cannot be captured by the DFT calculations which are valid only at $T = 0$. Under strain, the two bands with dominant d_{yz} and d_{xz} character become non-degenerate, and develop a finite splitting, Δ_{xz-yz} , at the X point in \mathbf{k} -space. We find that $\eta = A\Delta_{xz-yz}$, where $A = 5.7/\text{eV}$. These values are consistent with angle-resolved photoemission experiments that indicate a splitting $\Delta_{xz-yz} \sim 40$ meV in the nematic phase [5], whereas NMR studies reveal a value of $\eta \sim 1.2$ [21].

Fig. 2 also shows the quadrupolar splitting ν_{zz} along the c -axis to in-plane strain. This independent component of the EFG tensor does not couple to the nematic order, but nevertheless it is suppressed by the lattice distortion. We find that $|\nu_{zz}(\varepsilon_{ani})/\nu_{zz}(0)| = 1 - \beta\varepsilon_{ani}^2$, where $\beta \approx 9000$ is approximately temperature indepen-

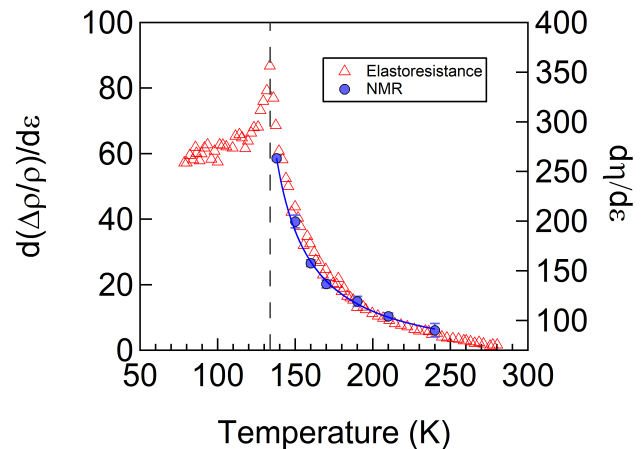


FIG. 4. (color online) The nematic susceptibility measured by the EFG asymmetry (\bullet) and that measured by elastoresistance (Δ , reproduced from [3]). The solid line is a fit to the NMR data, as described in the text. The vertical dashed line indicates T_N .

dent. Our DFT calculations reveal a small quadratic suppression with $\beta = 30$, due to changes in the relative occupations of the As p_z and $p_{x,y}$ orbitals. The difference between the experimental and theoretical values may reflect changes to the c -axis lattice parameters due to a finite Poisson ratio.

Our measurements offer insight into the behavior of the EFG in electron-doped pnictides. In doped $\text{Ba}(\text{Fe},\text{M})_2\text{As}_2$ ($\text{M} = \text{Co}, \text{Ni}$), the quadrupolar satellite resonances are inhomogeneously broadened ($\sim 1.0 - 1.5$ MHz) relative to those in the parent compound (0.13 MHz) [31–33]. A large source of this broadening may arise from local strain distributions. Local strains at dopant atoms can reach up to 3% [34], which would correspond to a shift in the As EFG parameters of $\delta\eta \sim 10$ and $\delta\nu_{zz} \sim 2.9$ MHz at 140 K. The strain field relaxes with distance from the dopant giving rise to a distribution of local EFGs. Recently a finite EFG asymmetry $\eta \sim 0.1$ was reported in $\text{BaFe}_2(\text{As}_{1-x}\text{P}_x)_2$ in the tetragonal phase [20]. This value would be consistent with an average strain field on the order of 0.05%. We postulate, therefore, that the origin of the finite nematicity observed in this compound reflects inhomogeneous strain fields from the dopant atoms, rather than intrinsic nematicity above the structural transition [35]. Complex EFG distributions have also been reported in $\text{RFeAsO}_{1-x}\text{F}_x$ ($\text{R} = \text{La}, \text{Sm}$) that have been interpreted as nanoscale electronic order [36]. It is unclear whether these spatial variations arise due to ν_{zz} or η , although they may reflect a combination of both strain and/or orbital occupations.

In conclusion, we have conducted detailed measurements of the EFG under a uniform uniaxial stress, and observed a linear response that is strongly temperature dependent. The slope agrees well with other measure-

ments of the nematic susceptibility, and demonstrates that C_4 symmetry is broken not only in the different Fe 3d orbital occupations, but also in the As 4p orbitals. Our results further demonstrate that ^{75}As NMR is sensitive to the charge degrees of freedom, and enable a quantitative measure of the local orbital occupations of the Fe d-orbitals. Measurements of the local nematicity by NMR provide an important microscopic complement to other techniques, and offer a unique opportunity to measure the response in the superconducting state. For example, in contrast to elasto-resistance and Raman scattering, NMR under strain can probe the nematic susceptibility below T_c . Such measurements may provide insight into the role of nematic degrees of freedom in the superconducting mechanism [37].

We thank S. Hillbrand, K. Delong, D. Hemer and P. Klavins, for assistance in the laboratory, and E. Carlson and I. R. Fisher for stimulating discussions. Work at UC Davis was supported by the NSF under Grant No. DMR-1506961 (T.K., M.L., B.T.B., N.J.C). NSF grant DMR-1607139 (W.F.G), DOE NNSA grant DE-NA0002908 grant (W.E.P.). R.M.F. is supported by the U. S. Department of Energy, Office of Science, Basic Energy Sciences, under award number DE-SC0012336. R.S. was partially supported by the DFG through SFB 1143 for the project C02. Work done at Ames Lab (S.L.B., P.C.C., M.T., R.P., E.I.T.) was supported by the U.S. Department of Energy, Office of Basic Energy Science, Division of Materials Sciences and Engineering. Ames Laboratory is operated for the U.S. Department of Energy by Iowa State University under Contract No. DE-AC02-07CH11358.

-
- [1] Paul C. Canfield and Sergey L. Bud'ko, "FeAs-based superconductivity: A case study of the effects of transition metal doping on BaFe_2As_2 ," *Annu. Rev. Condens. Matter Phys.* **1**, 27–50 (2010).
- [2] R. M. Fernandes, A. V. Chubukov, J. Knolle, I. Eremin, and J. Schmalian, "Preemptive nematic order, pseudogap, and orbital order in the iron pnictides," *Phys. Rev. B* **85**, 024534 (2012).
- [3] Jiun-Haw Chu, Hsueh-Hui Kuo, James G. Analytis, and Ian R. Fisher, "Divergent nematic susceptibility in an iron arsenide superconductor," *Science* **337**, 710–712 (2012).
- [4] T. Kissikov, A. P. Dioguardi, E. I. Timmons, M. A. Tanatar, R. Prozorov, S. L. Bud'ko, P. C. Canfield, R. M. Fernandes, and N. J. Curro, "NMR study of nematic spin fluctuations in a detwinned single crystal of underdoped $\text{Ba}(\text{Fe}_{1-x}\text{Co}_x)_2\text{As}_2$," *Phys. Rev. B* **94**, 165123 (2016).
- [5] M Yi, D H Lu, R G Moore, K Kihou, C-H Lee, A Iyo, H Eisaki, T Yoshida, A Fujimori, and Z-X Shen, "Electronic reconstruction through the structural and magnetic transitions in detwinned NaFeAs ," *New J. Phys.* **14**, 073019 (2012).
- [6] M. A. Tanatar, E. C. Blomberg, A. Kreyssig, M. G. Kim, N. Ni, A. Thaler, S. L. Bud'ko, P. C. Canfield, A. I. Goldman, I. I. Mazin, and R. Prozorov, "Uniaxial-strain mechanical detwinning of CaFe_2As_2 and BaFe_2As_2 crystals: Optical and transport study," *Phys. Rev. B* **81**, 184508 (2010).
- [7] Jiun-Haw Chu, James G. Analytis, Kristiaan De Greve, Peter L. McMahon, Zahirul Islam, Yoshihisa Yamamoto, and Ian R. Fisher, "In-plane resistivity anisotropy in an underdoped iron arsenide superconductor," *Science* **329**, 824–826 (2010).
- [8] W.-L. Zhang, Athena S. Sefat, H. Ding, P. Richard, and G. Blumberg, "Stress-induced nematicity in EuFe_2As_2 studied by raman spectroscopy," *Phys. Rev. B* **94**, 014513 (2016).
- [9] A. E. Böhmer, T. Arai, F. Hardy, T. Hattori, T. Iye, T. Wolf, H. v. Löhneysen, K. Ishida, and C. Meingast, "Origin of the tetragonal-to-orthorhombic phase transition in FeSe: A combined thermodynamic and NMR study of nematicity," *Phys. Rev. Lett.* **114**, 027001 (2015).
- [10] Mingquan He, Liran Wang, Felix Ahn, Frdric Hardy, Thomas Wolf, Peter Adelman, Jrg Schmalian, Ilya Eremin, and Christoph Meingast, "Dichotomy between in-plane magnetic susceptibility and resistivity anisotropies in extremely strained BaFe_2As_2 ," (2), 1610.05575v2.
- [11] Anna E. Böhmer and Christoph Meingast, "Electronic nematic susceptibility of iron-based superconductors," *C. R. Phys.* **17**, 90 – 112 (2016).
- [12] E. C. Blomberg, A. Kreyssig, M. A. Tanatar, R. M. Fernandes, M. G. Kim, A. Thaler, J. Schmalian, S. L. Bud'ko, P. C. Canfield, A. I. Goldman, and R. Prozorov, "Effect of tensile stress on the in-plane resistivity anisotropy in BaFe_2As_2 ," *Phys. Rev. B* **85**, 144509 (2012).
- [13] M. A. Tanatar, A. E. Böhmer, E. I. Timmons, M. Schütt, G. Drachuck, V. Taufour, K. Kothapalli, A. Kreyssig, S. L. Bud'ko, P. C. Canfield, R. M. Fernandes, and R. Prozorov, "Origin of the resistivity anisotropy in the nematic phase of FeSe," *Phys. Rev. Lett.* **117**, 127001 (2016).
- [14] C. Mirri, A. Dusza, S. Bastelberger, M. Chinotti, L. Degiorgi, J.-H. Chu, H.-H. Kuo, and I. R. Fisher, "Origin of the resistive anisotropy in the electronic nematic phase of BaFe_2As_2 revealed by optical spectroscopy," *Phys. Rev. Lett.* **115**, 107001 (2015).
- [15] F. L. Ning, M. Fu, D. A. Torchetti, T. Imai, A. S. Sefat, P. Cheng, B. Shen, and H.-H. Wen, "Critical behavior of the spin density wave transition in underdoped $\text{Ba}(\text{Fe}_{1-x}\text{Co}_x)_2\text{As}_2$ ($x \leq 0.05$): ^{75}As NMR investigation," *Phys. Rev. B* **89**, 214511 (2014).
- [16] T. Kissikov, R. Sarkar, M. Lawson, B. T. Bush, E. I. Timmons, M. A. Tanatar, R. Prozorov, S. L. Bud'ko, P. C. Canfield, R. M. Fernandes, and N. J. Curro, "Uniaxial strain control of spin-polarization in multicomponent nematic order of BaFe_2As_2 ," submitted to Nature Comm. (2017), 1704.03566v1.
- [17] Pengcheng Dai, "Antiferromagnetic order and spin dynamics in iron-based superconductors," *Rev. Mod. Phys.* **87**, 855–896 (2015).
- [18] Haoran Man, Xingye Lu, Justin S. Chen, Rui Zhang, Wenliang Zhang, Huiqian Luo, J. Kulda, A. Ivanov, T. Keller, Emilia Morosan, Qimiao Si, and Pengcheng Dai, "Electronic nematic correlations in the stress-free

- tetragonal state of $\text{BaFe}_{2-x}\text{Ni}_x\text{As}_2$,” *Phys. Rev. B* **92**, 134521 (2015).
- [19] Xingye Lu, J. T. Park, Rui Zhang, Huiqian Luo, Andriy H. Nevidomskyy, Qimiao Si, and Pengcheng Dai, “Nematic spin correlations in the tetragonal state of uniaxial-strained $\text{BaFe}_{2-x}\text{Ni}_x\text{As}_2$,” *Science* **345**, 657–660 (2014).
- [20] Tetsuya Iye, Marc-Henri Julien, Hadrien Mayaffre, Mladen Horvatić, Claude Berthier, Kenji Ishida, Hiroaki Ikeda, Shigeru Kasahara, Takasada Shibauchi, and Yuji Matsuda, “Emergence of orbital nematicity in the tetragonal phase of $\text{BaFe}_2(\text{As}_{1-x}\text{P}_x)_2$,” *J. Phys. Soc. Jpn.* **84**, 043705 (2015).
- [21] Kentaro Kitagawa, Naoyuki Katayama, Kenya Ohgushi, Makoto Yoshida, and Masashi Takigawa, “Commensurate itinerant antiferromagnetism in BaFe_2As_2 : ^{75}As -NMR studies on a self-flux grown single crystal,” *J. Phys. Soc. Jpn.* **77**, 114709 (2008).
- [22] T. Kissikov, R. Sarkar, B. T. Bush, M. Lawson, P. C. Canfield, and N. J. Curro, “Nuclear magnetic resonance probe head design for precision strain control,” *Rev. Sci. Instrum.* **88**, 103902 (2017).
- [23] A. P. Dioguardi, T. Kissikov, C. H. Lin, K. R. Shirer, M. M. Lawson, H.-J. Grafe, J.-H. Chu, I. R. Fisher, R. M. Fernandes, and N. J. Curro, “NMR evidence for inhomogeneous nematic fluctuations in $\text{BaFe}_2(\text{As}_{1-x}\text{P}_x)_2$,” *Phys. Rev. Lett.* **116**, 107202 (2016).
- [24] Hsueh-Hui Kuo, Jiun-Haw Chu, Johanna C. Palmstrom, Steven A. Kivelson, and Ian R. Fisher, “Ubiquitous signatures of nematic quantum criticality in optimally doped Fe-based superconductors,” *Science* **352**, 958–962 (2016).
- [25] N. Ni, S. L. Bud’ko, A. Kreyssig, S. Nandi, G. E. Rustan, A. I. Goldman, S. Gupta, J. D. Corbett, A. Kracher, and P. C. Canfield, “Anisotropic thermodynamic and transport properties of single-crystalline $\text{Ba}_{1-x}\text{K}_x\text{Fe}_2\text{As}_2$ ($x = 0$ and 0.45),” *Phys. Rev. B* **78**, 014507 (2008).
- [26] Y. Gallais, R. M. Fernandes, I. Paul, L. Chauvière, Y.-X. Yang, M.-A. Méasson, M. Cazayous, A. Sacuto, D. Colson, and A. Forget, “Observation of incipient charge nematicity in $\text{Ba}(\text{Fe}_{1-x}\text{Co}_x)_2\text{As}_2$,” *Phys. Rev. Lett.* **111** (2013), 10.1103/PhysRevLett.111.267001.
- [27] V. K. Thorsmølle, M. Khodas, Z. P. Yin, Chenglin Zhang, S. V. Carr, Pengcheng Dai, and G. Blumberg, “Critical quadrupole fluctuations and collective modes in iron pnictide superconductors,” *Phys. Rev. B* **93**, 054515 (2016).
- [28] Yann Gallais and Indranil Paul, “Charge nematicity and electronic raman scattering in iron-based superconductors,” *C. R. Phys.* **17**, 113–139 (2016).
- [29] H-J Grafe, G. Lang, F. Hammerath, D. Paar, K. Manthey, K. Koch, H. Rosner, N. J. Curro, G. Behr, J. Werner, N. Leps, R. Klingeler, H-H Klauss, F. J. Litterst, and B. Buechner, “Electronic properties of $\text{LaO}_{1-x}\text{F}_x\text{FeAs}$ in the normal state probed by NMR/NQR,” *New J. Phys.* **11**, 035002 (2009).
- [30] J. Cui, Q. P. Ding, W. R. Meier, A. E. Bhmer, T. Kong, V. Borisov, Y. Lee, S. L. Bud’ko, R. Valent, P. C. Canfield, and Y. Furukawa, “Magnetic fluctuations and superconducting properties of $\text{CaKFe}_4\text{As}_4$ studied by ^{75}As NMR,” (2017), 1706.09075v1.
- [31] F. L. Ning, K. Ahilan, T. Imai, A. S. Sefat, R. Jin, M. A. McGuire, B. C. Sales, and D. Mandrus, “ ^{59}Co and ^{75}As NMR investigation of lightly doped $\text{Ba}(\text{Fe}_{1-x}\text{Co}_x)_2\text{As}_2$ ($x = 0.02, 0.04$),” *Phys. Rev. B* **79**, 140506 (2009).
- [32] A. P. Dioguardi, N. apRoberts Warren, A. C. Shockley, S. L. Bud’ko, N. Ni, P. C. Canfield, and N. J. Curro, “Local magnetic inhomogeneities in $\text{Ba}(\text{Fe}_{1-x}\text{Ni}_x)_2\text{As}_2$ as seen via As-75 NMR,” *Phys. Rev. B* **82**, 140411(R) (2010).
- [33] Hikaru Takeda, Takashi Imai, Makoto Tachibana, Jonathan Gaudet, Bruce D. Gaulin, Bayrammurad I. Saporov, and Athena S. Sefat, “Cu substitution effects on the local magnetic properties of $\text{Ba}(\text{Fe}_{1-x}\text{Cu}_x)_2\text{As}_2$: A site-selective ^{75}As and ^{63}Cu NMR study,” *Phys. Rev. Lett.* **113**, 117001 (2014).
- [34] Keeseong Park, Despina Louca, Anna Llobet, and J.-Q. Yan, “Evidence of local disorder in the overdoped regime of $\text{Ba}(\text{Fe}_{1-x}\text{Co}_x)_2\text{As}_2$,” *Phys. Rev. B* **84**, 024512 (2011).
- [35] S. Kasahara, H. J. Shi, K. Hashimoto, S. Tonegawa, Y. Mizukami, T. Shibauchi, K. Sugimoto, T. Fukuda, T. Terashima, Andriy H. Nevidomskyy, and Y. Matsuda, “Electronic nematicity above the structural and superconducting transition in $\text{BaFe}_2(\text{As}_{1-x}\text{P}_x)_2$,” *Nature* **486**, 382–385 (2012).
- [36] G. Lang, H.-J. Grafe, D. Paar, F. Hammerath, K. Manthey, G. Behr, J. Werner, and B. Büchner, “Nanoscale electronic order in iron pnictides,” *Phys. Rev. Lett.* **104**, 097001 (2010).
- [37] S. Lederer, Y. Schattner, E. Berg, and S. A. Kivelson, “Enhancement of superconductivity near a nematic quantum critical point,” *Phys. Rev. Lett.* **114**, 097001 (2015).